processes

MDPI

Article

Location Distribution of Lightning Localization Monitoring Stations Integrating 3D Monitoring and PSO Algorithm

Yiming Han, Bin He and Hongchun Shu *

School of Electric Power Engineering, Kunming University of Science and Technology, Kunming 650500, China; kmhym1993@sina.com (Y.H.); hebin@stu.kust.edu.cn (B.H.)
* Correspondence: lwj_kust@sina.com

Abstract: The growth of the modern information technology sector and the safe use of electrical equipment depend on accurate lightning localization monitoring. However, along with the increase in the number of lightning localization equipment and monitoring stations, the unreasonable station location distribution increases the risk of error in lightning localization monitoring. Therefore, the study integrates three-dimensional cross-location lightning monitoring and particle swarm algorithm to optimize the multi-station location distribution of lightning localization monitoring. In the simulation experiment of the four-station lightning monitoring system, compared with the traditional Y-distribution method, the particle swarm optimization method reduced the lightning positioning error by 45.8%. Meanwhile, in the practical application analysis, the positioning error of the proposed method in the horizontal and vertical axes was basically less than 0.4 km, which was the smallest compared with other models. The experiment proves that the lightning localization monitoring station distribution method fusing 3D localization and PSO algorithm constructed by the research has good location distribution performance and can be effectively applied to the layout of the current multi-station lightning monitoring system.

Keywords: lightning localization; cross-localization method; particle swarm algorithm; geometrical dilution of precision; monitoring station

check for updates

Received: 11 October 2024
Revised: 12 November 2024
Accepted: 17 December 2024
Published: 24 December 2024

Citation: Han, Y.; He, B.; Shu, H. Location Distribution of Lightning Localization Monitoring Stations Integrating 3D Monitoring and PSO Algorithm. *Processes* **2025**, *13*, 2. https://doi.org/10.3390/pr13010002

Copyright: © 2024 by the authors. Licensee MDPI, Basel, Switzerland. This article is an open access article distributed under the terms and conditions of the Creative Commons Attribution (CC BY) license (https://creativecommons.org/licenses/by/4.0/).

1. Introduction

As a kind of natural, strong electromagnetic phenomenon, lightning occurs with high voltage and electromagnetic radiation, which will affect the safety of information communication, aerospace, electric power and petrochemical equipment. Lightning phenomena without accurate localization monitoring can easily cause economic losses in the information industry and casualties in various industrial fields [1]. Lightning Localization (LL) monitoring is the current research focus of natural disaster protection in the information field. The effectiveness of LL is significantly impacted by the distribution design of lightning monitoring stations [2]. However, with the development of information facility infrastructure throughout the country, large-scale lightning monitoring needs to rely on multiple sites to detect and return lightning weather phenomena in the same area [3]. Therefore, exploring the optimal location distribution of multiple lightning signal detection stations is crucial to improving the accuracy of the lightning detection network. Intelligent optimization algorithms have potential in LL and station deployment optimization. In particular, they can provide effective solutions when dealing with complex optimization problems [4]. The study employs a particle swarm intelligent optimization technique to maximize the distribution of lightning monitoring stations, while standard positioning

methods are susceptible to the influence of site layout. The latest trend in lightning monitoring technology is focused on improving the continuity, real-time performance, and accuracy of detection, as well as developing and applying new detection techniques and algorithms to better understand and warn of severe convective weather. The study proposes to integrate the 3D monitoring and Particle Swarm Optimization (PSO) algorithms with the aim of planning lightning detection stations more scientifically, thus improving the accuracy of LL. The innovation of the study is that PSO is introduced into the 3D boda direction localization technique, which improves the performance of the boda direction localization technique and provides theoretical and practical support for the development of the current multi-site lightning monitoring system.

An overview of the boda orientation localization method and the PSO location distribution application is given in Section 1 of the study. The second part demonstrates in detail the construction of the optimization method for the location distribution of the LL monitoring stations by integrating the 3D monitoring and PSO algorithms. The third part analyzes the comparative experiments of the methods constructed in the study. The results of the study are summarized in the conclusion of the fourth part.

2. Related Work

The LL technique is the current research focus in the field of information and communication because the localization of lightning is closely related to communication quality and safety issues. Li et al. utilized Time Difference of Arrival (TDOA) and Angle of Arrival (AOA) for binary star localization. The experiment proved that the AOA localization algorithm was feasible and had stable performance [5]. Chen et al. introduced the time reversal technique into lightning 3D localization and proposed a new 3D localization algorithm for lightning low-frequency discharges. In the experiment, the localization deviation of this method in both X and Y directions of the lightning return stroke was about 90 m [6]. Qin et al. used a parallel computing algorithm with a graphics processing unit for LL. The process might create a geolocation database beforehand using the numerical solution of a whole model and then use a grid search method to quickly and accurately estimate the lightning's location in real-time. In experiments, the method was approximately 2700 times faster than the traditional grid traversal localization method. Meanwhile, the technique demonstrated high-precision real-time lightning source location in Monte Carlo simulation studies [7]. Wang et al. proposed two Geometrical Dilution of Precision (GDOP) methods, discussed conical configurations with minimum GDOP, and extended them to ultra-wideband localization. Simulation findings showed that the approach might efficiently optimize anchor deployment by taking constraint statistics into account while optimizing the global GDOP distribution in the localization region [8]. Tirkolaee et al. found that lightning typically has multiple grounding endpoints and, therefore, analyzed the spatiotemporal patterns of European GSP from 2013 to 2022 using the European Lightning Detection Cooperation Organization combined with ground strike point algorithms. The results show that GSP density varies on the European continent, with high densities in the Mediterranean, Adriatic, and Baltic regions, and the GSP numbers peak from September to November [9]. Goeritno and Azama used achievement and persistence algorithms for cloud and lightning formation, electromagnetic field measurement principles, and lightning detection systems, which were explained through a literature review and flowcharts. Discussed three main issues: cloud formation, electromagnetic field measurement, and lightning strike detection [10]. Nahar and Mostafa conducted a statistical analysis of lightning activity in Bangladesh based on global lightning location network data from 2020 to 2023. During this period, 2.06 million lightning strikes were recorded, and annual and seasonal lightning density peaks were found, mainly concentrated in the

north and northeast. The number of lightning strikes is highest in June, and the activity is most frequent at 20:00 at night [11].

Among the methods and metrics used in the study, geometric accuracy dilution is often used in current location distribution studies. Poelman et al. constructed an optimization method for product location distribution using PSO, taking into account issues such as traffic environment and transportation cost. In the experiment, the average gap of the method was 0.9%, which indicated that the method has excellent performance in product location optimization [12]. Wang et al. utilized the PSO algorithm to optimize the battery location distribution in the PV grid. In the experiments, the PSO algorithm demonstrated good location distribution performance, which minimized both the PV network power loss and node voltage fluctuations [13]. Rafi and Dhal used the PSO algorithm and Dragonfly algorithm to simultaneously reconfigure the distribution network and identify optimal installation locations. This technique used the Dragonfly method to determine the best position for the dispersed generating units and applied the PSO method to the reconfiguration of the distribution network [14]. Mehranzamir et al. used the PSO algorithm to localize cloud-to-ground lightning and determine the optimal location of lightning strikes. In experiments, the method had an average error of 573 m and effectively and accurately detected and mapped lightning discharges occurring in the coverage area [15]. Zhang et al. discussed the development trend of lightning monitoring from one station to multiple stations. The study also analyzed the future research direction of lightning mapping imagers for geosynchronous satellites [16].

In summary, most of the current site distribution optimization methods for LL monitoring focus on site optimization within a small area, with relatively weak performance for site distribution in complex terrain or large areas. Meanwhile, some of the algorithms have defects in computational volume and generalizability. Therefore, PSO combined with three-dimensional cross-location is used to construct a multi-station location distribution optimization method for lightning monitoring.

3. Optimization of Monitoring Station Location Distribution for Lightning Localization by Integrating 3D Monitoring and PSO Algorithm

The study plans the location distribution of lightning monitoring sites with the accuracy of LL of multiple sites as the core index. In the study, the cross-location method is first adopted to realize the LL of 3D monitoring. On this basis, the PSO fusion 3D cross-location method is utilized to solve the problem of optimal station location distribution.

3.1. Lightning Localization Model Based on 3D Monitoring

Three-dimensional monitoring of LL requires the synergy of three components: the monitoring station, the data processing system, and the workstation. The monitoring station is responsible for receiving lightning signals, while the data processing system is engaged in analyzing the data, such as the time, location, and intensity of the lightning return strokes transmitted from the monitoring station [17]. The specific LL monitoring system for 3D monitoring is shown in Figure 1.

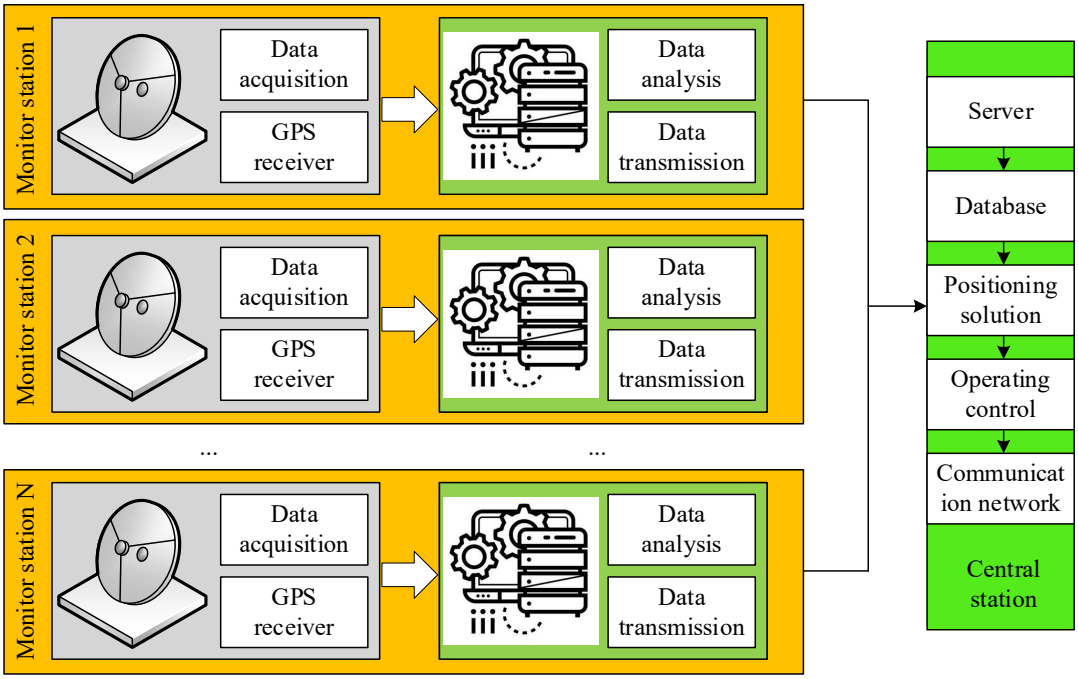

Figure 1. Lightning localization monitoring system for three-dimensional monitoring.

In Figure 1, the height information of the lightning transmitting source and the height information of the monitoring station possess an influence on the accuracy of localization, so it is necessary to construct a three-dimensional wave direction interaction space on the basis of the two-dimensional wave direction interaction points. In passive 3D positioning technology, Time Difference of Arrival (TDOA) and Angle of Arrival (AOA) algorithms are widely used. TDOA is located by comparing the relative time of signals emitted by signal sources reaching two or more receiving stations. Since signal sources are non-cooperative, each receiving station needs to communicate with the other and share the data it receives with other receiving stations. AOA detects the direction of arrival of multiple receiving stations for the same signal and then obtains the coordinate information of the signal source by calculating the intersection points of multiple lines. Therefore, the multi-station localization method adopted in the study mainly relies on AOA for three-dimensional monitoring [18]. Thus, the intersection point of the straight line in the wave direction is used to infer the localization of lightning occurrence, as shown in Figure 2.

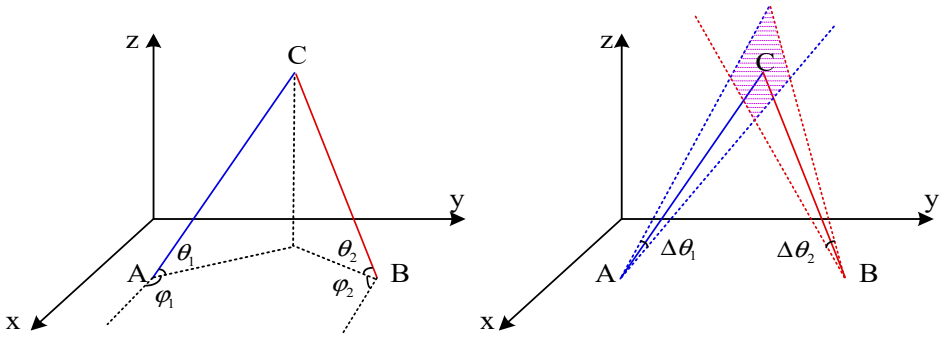

(a) Three dimensional monitoring cross localization method

(b) The error space of three-dimensional monitoring cross localization

Figure 2. Three-dimensional cross localization and error space.

In Figure 2b, when the height information is added, the interaction point formed by the boda direction becomes the intersection space, which leads to the error space for the

localization of lightning emission sources. Especially when affected by terrain with height differences, such as mountains and depressions, the signal acquisition will be affected by errors, resulting in inaccurate positioning. Therefore, the study decomposes the signal positioning error caused by terrain into three-axis errors by introducing Geometric Dilution of Precision (GDOP) to describe the relationship between error and position, thereby increasing positioning accuracy. To make it easier to investigate the connection between the monitoring stations' locations and the positioning inaccuracy caused by lightning, the study first adopts a two-site cross-location method for model construction and then expands to a multi-site network location optimization afterward.

Assuming that site $A(x_1, y_1, z_1)$ and site $B(x_2, y_2, z_2)$ are laterally oriented to the lightning signal source $C(x, y, z)$, the set of boda direction from the lightning signal source C at site A can be defined as $DOA_{A\to C}(\varphi_1, \theta_1)$. Similarly, the set of boda direction from the lightning signal source C at site A can be defined as $DOA_{B\to C}(\varphi_2, \theta_2)$. The lightning signal source with point A produces ray 1 with an azimuth angle of φ_1 and a pitch angle of θ_1. Moreover, the lightning signal source with point B produces ray 2 formed by an azimuth angle of φ_2 and a pitch angle of θ_2. The intersecting position (x, y, z) of ray 1 and ray 2 is the lightning signal source position. Among them, the azimuth angle calculation formula is shown in Equation (1).

$$\begin{cases} \tan\varphi_1 = \frac{y-y_1}{x-x_1} \\ \tan\varphi_2 = \frac{y-y_2}{x-x_2} \\ \tan\theta_1 = \frac{z-z_1}{\sqrt{((y-y_1)^2+(x-x_1)^2)}} \\ \tan\theta_2 = \frac{z-z_2}{\sqrt{((y-y_2)^2+(x-x_2)^2)}} \end{cases} \tag{1}$$

In Equation (1), φ denotes the azimuth angle and θ denotes the pitch angle. From the trigonometric formula (1) for azimuth, the following Equation (2) can be derived.

$$\begin{cases} y - x\tan\varphi_1 = -x\tan\varphi_1 + y_1 \\ y - x\tan\varphi_2 = -x\tan\varphi_2 + y_2 \end{cases} \tag{2}$$

Similarly, the following Equation (3) can be derived from the formula $\tan\theta_1 = (z - z_1)/(y - y_1)$ for pitch angle θ.

$$\begin{cases} -z\sin\varphi_1 + y\tan\theta_1 = -z_1\sin\varphi_1 + y_1\tan\theta_1 \\ -z\sin\varphi_2 + y\tan\theta_2 = y_2\tan\theta_2 - z_1\sin\varphi_2 \end{cases} \tag{3}$$

Equation (2) as well as Equation (3) are represented as matrices according to the simplified form of $HX = Z$. H is denoted as a matrix of coefficients, specifically denoted in the study as the trigonometric function values associated with the angle. X denotes the unknown term vector, specifically denoted in the study as the position coordinate matrix of the lightning signal source. Z is the known term vector. The matrix derived from this form is shown in Equation (4).

$$\begin{bmatrix} -\tan\varphi_1 & 1 & 0 \\ 0 & \tan\theta_1 & -\sin\varphi_1 \\ -\tan\varphi_2 & 1 & 0 \end{bmatrix} \begin{bmatrix} x \\ y \\ z \end{bmatrix} = \begin{bmatrix} y_1 - x_1\tan\varphi \\ y_1\tan\theta_1 - z_1\sin\varphi_1 \\ y_2 - x_2\tan\varphi_2 \end{bmatrix} \tag{4}$$

After deriving the matrix, the matrix form of $HX = Z$ can be transformed into $X = H^{-1}Z$, so that the positioning coordinates of the lightning signal source can be calculated. Furthermore, the relationship between the positioning error of the lightning

signal source and the spatial location of the monitoring station point must be described by geometrical dilution of precision (GDOP). This allows the error optimization problem of lightning 3D positioning to be transformed into the optimization problem of the distribution of the spatial location of the monitoring station. The calculation formula of GDOP is shown in Equation (5).

$$GDOP = \sqrt{\sigma_x^2 + \sigma_y^2 + \sigma_z^2} \tag{5}$$

In Equation (5), $GDOP$ denotes the GDOP and σ denotes the positioning error in the three-axis direction. In order to ensure that the measurement errors (MEs) are independent of each other and the uncertainty level of each error is consistent, it is necessary to assume that the MEs are zero-mean and uncorrelated with each other and that the Gaussian white noise has the same standard deviation (SD) $(\sigma_\varphi, \sigma_\theta)$. At the same time, the MEs of different stations are relatively independent of each other and have the same SD σ_s. σ_φ, σ_θ, and σ_s denote the azimuthal, pitch, and positional SDs of the MEs, respectively. Differential equations are used to assess the relationship between the ME and the fluctuation of position parameters. Firstly, differentials are taken on both sides of Equations (2) and (3) to obtain the following Equation (6).

$$\begin{cases} df_1 = \frac{\sin^2 f_1}{y-y_1}dx + \frac{\cos^2 f_1}{x-x_1}dy + k_{\varphi 1} \\ d\theta_1 = -\frac{(z-z_1)\cos\varphi_1}{r_1^2}dx - \frac{(z-z_1)\sin\varphi_1}{r_1^2}dy + \frac{\cos\theta_1}{r_1}dz + k\theta_2 \\ d\varphi_2 = -\frac{\sin^2\varphi_2}{y-y_1}dx + \frac{\cos^2\varphi_2}{x-x_2}dy + k_{\theta 2} \end{cases} \tag{6}$$

In Equation (6), df_1 denotes the fine variation of the PDF of the monitoring station location. dx, dy and dz then denote the three-axis fine variations of the lightning source location. r_1 denotes the nonlinear distance between the lightning source and the monitoring station. f_1 denotes the probability density function (PDF) of the monitoring station location. The calculation method is expressed as the following Equation (7).

$$f(x,y) = \frac{1}{2\pi\sigma_x\sigma_y\sqrt{1-\rho^2}}\exp\left\{\frac{-1}{2(1-\rho^2)}\left[\frac{(x-\overline{x})^2}{\sigma_x^2} - 2\rho\frac{(x-\overline{x})(y-\overline{y})}{\sigma_x\sigma_y} + \frac{(y-\overline{y})^2}{\sigma_y^2}\right]\right\} \tag{7}$$

k denotes the scaled differential term, which is calculated as shown in Equation (8).

$$\begin{cases} k_{\varphi 1} = \frac{\sin^2\varphi_1}{y-y_1}dx - \frac{\cos^2\varphi}{x-x_2}dy \\ k_{\theta 1} = \frac{(z-z_1)}{r_1^2}dx + \frac{(z-z_1)}{r_1^2}dy - \frac{\cos\theta}{r_1}dz \end{cases} \tag{8}$$

To facilitate the linear method solution, Equation (6) is written in matrix form, as shown in Equation (9).

$$\begin{cases} dV = CdX + dX_s = (d\varphi_1, d\theta_1, d\varphi_2)^T \\ dX = (dx, dy, dz)^T \\ dX_s = (k_{\varphi 1}, k_{\theta 1}, k_{\varphi 2})^T \end{cases} \tag{9}$$

In Equation (9), dV denotes the observation error. dX denotes the lightning signal positioning error. dX_s denotes the monitoring station location positioning error. C denotes the coefficient matrix of lightning signal localization with respect to the distribution of monitoring station locations. The coefficient matrix is derived by expressing the relationship between observation error, positioning error, and the positioning error of the base station itself in matrix form. After obtaining the observation error vector, positioning error vector, and base station positioning error vector of the observation station from Equation (8),

the coefficient matrix is obtained by changing the target latitude and longitude. The elements of this matrix are functions of the target coordinates relative to the observation station coordinates. Specifically, each element represents how small changes in the target coordinates affect observation errors. The coefficient can be calculated from Equation (9), as shown in Equation (10).

$$C = \begin{bmatrix} -\frac{\sin^2\varphi_1}{y-y_1} & \frac{\cos^2\varphi_1}{x-x_1} & 0 \\ -\frac{(z-z_1)\cos\varphi_1}{r_1^2} & -\frac{(z-z_1)\sin\varphi_1}{r_1^2} & \frac{\cos\theta_1}{r_1} \\ -\frac{\sin^2\varphi_2}{y-y_2} & \frac{\cos^2\varphi_2}{x-x_2} & 0 \end{bmatrix} \tag{10}$$

Meanwhile, the covariance matrix (CM) between the lightning signal positioning error and the monitoring station location positioning error is expressed as the following Equation (11).

$$E[dX_s \cdot dX_s^T] = \begin{bmatrix} \frac{1}{[(x-x_1)^2+(y-y_1)^2]} & & \\ & \frac{1}{r_1^2} & \\ & & \frac{1}{[(x-x_2)^2+(y-y_2)^2]} \end{bmatrix} \tag{11}$$

In Equation (11), E denotes the CM. Based on this equation, the CM of the lightning signal positioning error can be derived as in Equation (12).

$$\begin{aligned} P_{dx} &= E[dx \cdot dx^T] = \mathrm{cov}(dx) = C^{-1}[\mathrm{cov}(dV - dx_s)][C^{-1}]^T \\ &= C^{-1}[\mathrm{cov}(dv) + \mathrm{cov}(dX_s)][C^{-1}]^T \\ &= C^{-1}\left\{E[dV \cdot dV^T] + E[dX_s \cdot dX_s^T]\right\}[C^{-1}]^T \\ &= C^{-1}\begin{bmatrix} \sigma_\varphi^2 + \frac{\sigma_s^2}{[(x-x_1)^2+(y-y_1)^2]} & & \\ & \sigma_\theta^2 + \frac{1}{r_1^2}\sigma_\theta^2 & \\ & & \sigma_\varphi^2 + \frac{\sigma_s^2}{[(x-x_2)^2+(y-y_2)^2]} \end{bmatrix} \end{aligned} \tag{12}$$

In Equation (12), cov denotes the covariance, which is used as a metric to measure whether the trends between different variables are the same or opposite. Equation (12) shows that the CM of the lightning signal's positioning error is derived under the calculation of the CM of the monitoring station positioning error transformed coefficient matrix C.

3.2. Optimization Algorithm for Lightning Localization Monitoring Multi-Site Distribution Location by Incorporating PSOs

A multi-site monitoring network is the core development direction of current LL technology. However, the multi-site monitoring system also faces the problem of optimal targets in the selection of site locations. Multiple monitoring stations can provide more data points, and through cross-validation and comparison, the location of lightning can be more accurately determined. At the same time, multiple monitoring stations can cover a wider geographical area, reduce monitoring blind spots, and improve the monitoring capability of lightning activity. When determining the number of stations in a multisite monitoring network, it is necessary to consider the size of the monitoring area, monitoring accuracy requirements, and economic costs.

The three-dimensional monitoring of LL is affected by the location and height of multiple stations. In the above 3D cross-localization method, the study mainly analyzes the relationship between the lightning signal positioning error and the monitoring station location distribution in the two-station case. Next, the study extends the two-station model

to a multi-station model. Firstly, one monitoring station is identified as the primary station, and the remaining stations are the auxiliary stations. A two-by-two cross-location of the primary and auxiliary stations is adopted to follow the two-station model described above. In the first cycle of cross-localization, assuming that the coordinates of the main station are $A(x_{00}, y_{00}, z_{00})$ and the coordinates of the remaining auxiliary stations are (x_{0i}, y_{0i}, z_{0i}), the lightning signal location derived from the cross-localization of the main station and any auxiliary station is $C(x_i, y_i, z_i)$. $N-1$ sets of lightning signal localization can be obtained in the first cycle of cross-localization. These localization data are processed using the maximum likelihood estimation method for optimal objective solving. The optimal objective of lightning signal localization is solved by PSO. After obtaining the optimal positioning objective, the location optimization of multi-station sites is solved based on the coefficient relationship between lightning signal positioning and monitoring station location distribution in the above model [19–21].

Firstly, according to the calculation method of azimuth and pitch angle in Equation (1), the equation of three-dimensional coordinates of lightning signals can be derived, as shown in Equation (13).

$$\begin{cases} x = \frac{(y_1-y_2)\tan\theta_1\tan\theta_2+x_2\tan\theta_1-x_1\tan\theta_2}{\tan\theta_1-\tan\theta_2} \\ y = \frac{x_2-x_1+y_1\tan\theta_1-y_2\tan\theta_2}{\tan\theta_1-\tan\theta_2} \\ z = z_1+\tan\varphi_1\sqrt{(x-x_1)^2+(y-y_1)^2} \end{cases} \tag{13}$$

Due to the ME, the rays of the two stations obtained from the actual measurement may not precisely intersect at one point but intersect in an area. Therefore, it is assumed that the random direction ME of the main station is $(\Delta\theta_1, \Delta\varphi_1)$, and the random lateral direction error of the auxiliary station is $(\Delta\theta_2, \Delta\varphi_2)$. Meanwhile, the azimuth and pitch angle errors of the main station are $N\left(0, \sigma_{\theta_1}^2\right)$ and $N\left(0, \sigma_{\varphi_1}^2\right)$, while those of the auxiliary station are $N\left(0, \sigma_{\theta_2}^2\right)$ and $N\left(0, \sigma_{\varphi_2}^2\right)$. When calculating the errors of the auxiliary station of the main station, the calculation of the azimuth and pitch angle needs to apply the square-open operation, which possesses a large nonlinear characteristic. Therefore, the PSO algorithm is used to solve the errors.

PSO sets the initialized random particles to obtain the optimal solution of the error value through the individual extremes as well as the global extremes in the iterative process. This is shown in Equation (14).

$$\begin{cases} V_i = \omega_i \cdot V_i + c_i \cdot rand() \cdot (P_i - x_i) + c_2 \cdot rand() \cdot (G_i - x_i) \\ x_i = x_i + V_i \end{cases} \tag{14}$$

In Equation (14), V_i denotes the velocity of particle movement. x_i denotes the particle position. ω_i denotes the inertia weights. c_i and c_2 are learning factors. P_i and G_i then denote the individual extremes and global extremes. Meanwhile, in order to evaluate the error results derived randomly by the particle swarm, the study defines the fitness function as shown in Equation (15).

$$F = |z_{1t} - z_{2t}| + \omega_1\left(\frac{\Delta\theta_1}{\sigma_{\theta_1}} + \frac{\Delta\varphi_1}{\sigma_{\varphi_1}}\right) + \omega_2\left(\frac{\Delta\theta_2}{\sigma_{\theta_2}} + \frac{\Delta\varphi_2}{\sigma_{\varphi_2}}\right) \tag{15}$$

In Equation (15), F denotes the fitness function. ω_1 and ω_2 denote the weight values. z_{1t} denotes the height of the monitoring station under the random error. z_{2t} denotes the measured monitoring station height, and the smaller the difference between the two, the closer the random error is to the real value. The reason why the height value of the station is used as an assessment index is that the angular error needs to be converted to the positional

error in the summation of the ratio of the estimated value of each random error to the SD of the systematic error. The angular deviation size is equal in status to the height deviation size in the fitness function. In Equation (15), the weight values are calculated as in Equation (16).

$$\begin{cases} \omega_1 = \frac{\sqrt{(y-y_1)^2+(x-x_1)^2}}{\Delta z} \\ \omega_2 = \frac{\sqrt{(y-y_2)^2+(x-x_2)^2}}{\Delta z} \end{cases} \tag{16}$$

In Equation (16), Δz denotes the error threshold for station height. In order to avoid the problem of the PSO algorithm getting stuck in local optima, this study dynamically adjusts the weight values and learning factors of the algorithm based on its current performance. The specific parameter adjustment is shown in Equation (17).

$$\begin{cases} \omega^{k+1} = \omega^k + \Delta\omega \\ c^{k+1} = c^k + \Delta c \end{cases} \tag{17}$$

In the formula, $\Delta\omega$ and Δc represent the increments of weights and learning factors, respectively. The increment is adjusted according to the rules of algorithm performance feedback. The process of PSO optimization to derive the monitoring station angle error data is as follows.

In Figure 3, after randomly setting the initial velocity and position of the particle, the position of the particle consists of the azimuth and pitch angle error values of the main and auxiliary stations. After the initialization work is completed, the altitude error of the monitoring station is used as the threshold value to define the adaptation function. In the process of particle updating, the fitness values of initialized particles and new particles are judged. The particle with smaller fitness is used as the new particle until the fitness value is less than the threshold value or the update iterations reach the maximum value. Finally, the pitch and azimuth errors are output, and the optimal localization of the lightning signal is calculated by Equation (12) after obtaining the angular data. The optimal localization of Equations (9)–(11) is calculated with the localization CM of the monitoring station to derive the optimal monitoring point location data. In the figure, P, G, Y, and N represent individual extremum global mechanisms, yes and no, respectively.

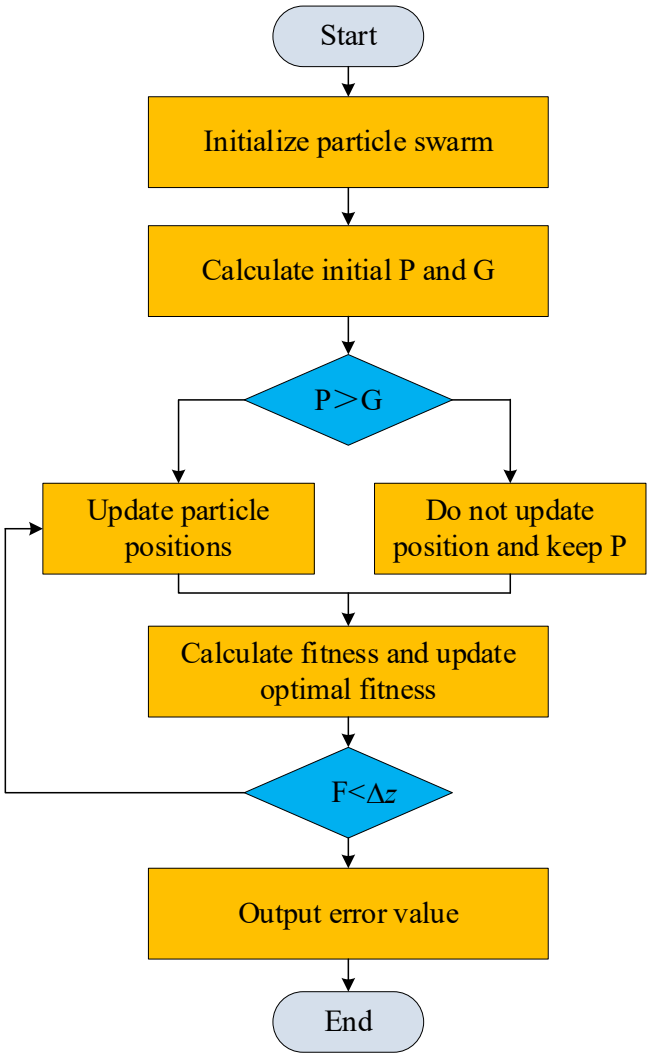

Figure 3. Particle swarm optimization process.

4. Experimental Analysis of Optimizing the Location Distribution of Multi-Site Lightning Monitoring Stations

In order to validate the optimization method of LL monitoring station location distribution that integrates 3D monitoring and the PSO algorithm constructed by the study, the study takes the standard four-station lightning monitoring network as the simulation object. The distribution of 16 stations in a provincial region is used as the actual experimental object. The study investigates the comparison of the positioning error between the proposed method and the traditional distribution and differential evolution methods.

4.1. Simulation of the Positional Distribution of the Four Stations

The study will be carried out in an intelligent monitoring station position optimization simulation system (IMS-POS) to optimize the location distribution of four stations for lightning monitoring. Table 1 displays the experimental parameters and environmental platform.

Table 1. Experimental parameters and environmental platform.

Algorithm Parameters	Value	Experimental Environment Project	Name
Initial particle count	40	CPU	Intel i7-7700K @4.2 GHz
Inertial weight	0.6–1	GPU	NVIDIA GTX 1080Ti
Individual learning factors	2	Memory	16 G
Social learning factors	2	platform	Intelligent monitoring station position optimization simulation system
Maximum number of iterations	500	Back-end	Python 3.8

Firstly, the error curves of the differential evolution method, as well as the PSO constructed by the study, are compared during one iteration. The population size and the maximum iterations of the differential evolution algorithm are the same as those of the PSO algorithm. Its scaling factor is 0.5, and the crossover probability is 0.2. Figure 4 displays the exact experimental results.

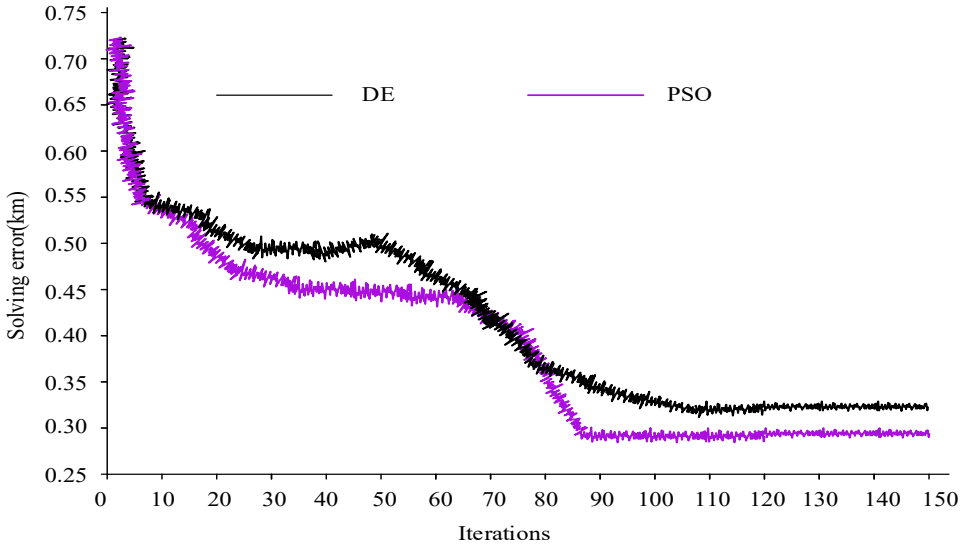

Figure 4. Error curves of different algorithms in iteration.

In Figure 4, the PSO basically completes convergence when the number of iterations reaches 90, and the solving error after that is basically stabilized at about 0.3 km. Moreover, the differential evolutionary algorithm completes the convergence when the number of iterations is about 110 times 2. The level of the solving error after convergence is at about 0.33 km. Therefore, the experiments show that there is not much difference between the two algorithms in terms of error in localization accuracy, but the PSO proposed by the study is better than the differential evolutionary algorithm in terms of convergence efficiency. Meanwhile, the study compares the GDOP distribution of the four-station distribution under the optimization of the two algorithms. The specific results are shown in Figure 5.

Taking the coordinates of the primary site as (0,0,0), under the optimization of the position part of the particle swarm, the coordinates of the remaining three auxiliary sites are distributed as (79.48, 100, 3), (−2.55, 84.18, 0.39), and (−89.55, 100, 3). Moreover, with the optimization of the differential evolutionary algorithm, the coordinates of the three auxiliary sites are (−88.91, 0, 0.05), (−100, 100, 3), and (−100, −100, 3). In Figure 5, the sparseness of the GDOP contour distribution is slightly higher than that of the GDOP contour distribution of the differential evolutionary algorithm under the optimization of the site distribution of PSO. Taking this experiment as the first iteration, four iterations of experiments are continued in the subsequent experiments. Comparing the positioning

errors of the two algorithms, the specific results are shown in Table 2. In this experiment, two traditional four-station distribution methods, T and Y, were used as comparative data for the traditional distribution. In a T-shaped distribution, with (0,0,0) as the center point, the coordinates of the four points are (100, 100, 0), (100, 120, 0), (80, 120, 0), and (120, 120, 0). The four-point coordinates of the Y-shaped distribution are (100, 100, 0), (117.32, 110, 0), (82.68, 110, 0), and (100, 80, 0).

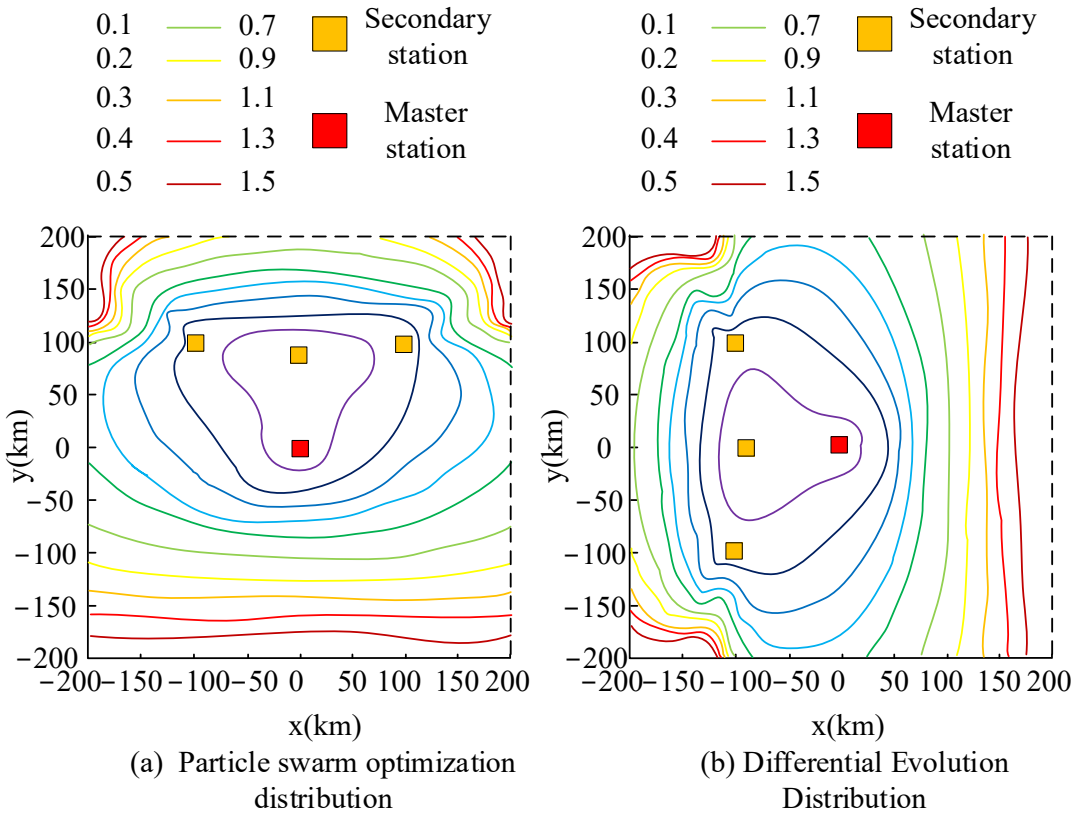

Figure 5. The GDOP distribution of four stations is optimized by two algorithms.

Table 2. Comparison table of lightning positioning errors for five iterations.

Algorithm Comparison	1	2	3	4	5
T-shaped distribution (km)	0.547	0.530	0.509	0.546	0.519
Y-shaped distribution (km)	0.569	0.563	0.568	0.563	0.561
DE (km)	0.328	0.327	0.325	0.326	0.327
PSO (km)	0.309	0.306	0.305	0.302	0.308

Table 2 shows that under the traditional T-shaped location distribution, the maximum error of LL is 0.546 km, the minimum is 0.509 km, and the average error is 0.5303 km. Under the traditional Y-shaped distribution method, the maximum error of LL is 0.569 km, the minimum is 0.561 km, and the average error is 0.5646 km. The average error is 0.5646 km. Under the distribution optimization of differential evolution, the lightning positioning error is a maximum of 0.328 km, a minimum of 0.325 km, and the average error is 0.3267 km. Under the distribution optimization of the particle swarm, the maximum lightning positioning error is 0.309 km, the minimum is 0.302 km, and the average error is 0.3057 km. Therefore, compared with the traditional Y-distribution method, the monitoring station optimized by the differential evolution method partially reduces the lightning positioning error by 42.1%. The PSO method reduces the lightning positioning error by 45.8% compared to the traditional Y-distribution method.

4.2. Practical Application of PSO to Optimize Position Distribution

The study takes Guangxi province as an example, where 16 lightning monitoring sites are planned to be placed. The study first uses a PSO-based optimization model to simulate on a provincial scale to find the optimal distribution of station locations. Before the experiment, the study used the meteorological bureau's planned monitoring network in the province as the basic information to ensure the height difference within the region. At the same time, local lightning data was collected during the thunderstorm weather from 12 June 2024 to 13 June 2024. The differential evolution method is also used for comparison. Lightning is assumed to occur at an altitude of 10 km in the experiment. Firstly, the speculation of the monitoring station location distribution of the two algorithms is shown in Figure 6.

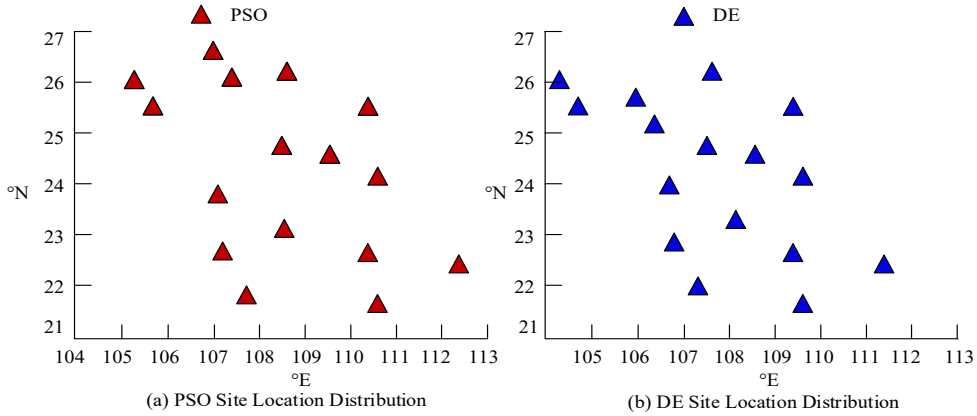

Figure 6. Two algorithms for predicting the location distribution of monitoring stations.

In Figure 6, 10 of the 16 sites marginalized by both algorithms are identical in terms of location distribution, and the remaining 6 sites biased toward the interior are partially different. Specifically, the PSO algorithm inferred that the lightning monitoring sites are farther away from each other than the site distances of the differential evolution algorithm. Therefore, the study will analyze the lightning positioning error at different station distances. The specific results are shown in Figure 7.

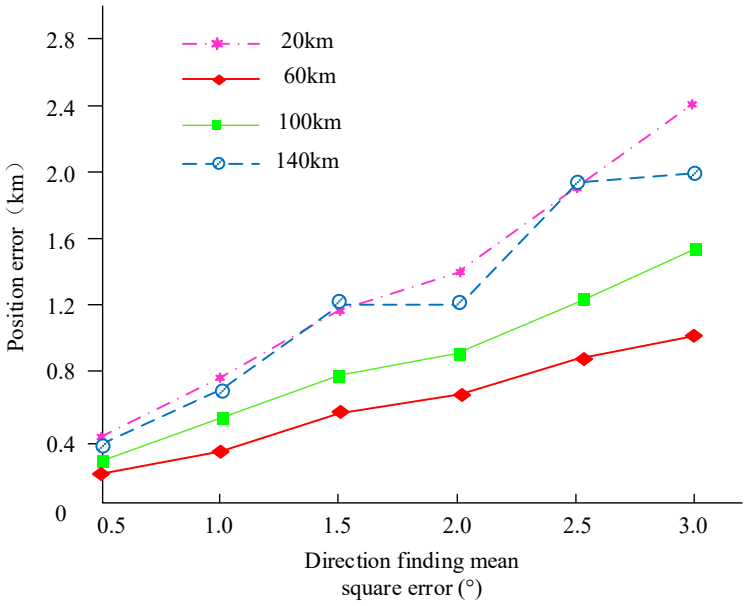

Figure 7. Changes in positioning error at different station distances.

In Figure 7, the error of the monitoring stations on the LL increases with the increase of the mean square error of the measurement direction between the stations. When the average distance between the stations is 20 km, the maximum error can reach 2.4 km. When the average distance between the stations is 140 km, the maximum positioning error of the monitoring station can reach 2.1 km. When the average distance between the stations is 60 km, the maximum error can reach 0.9 km. When the average distance between the stations is 100 km, the maximum positioning error of the monitoring station can reach 1.5 km. From the experimental results, it can be noted that in the range of 20–60 km, the longer the distance between monitoring stations, the higher the accuracy of LL. However, the accuracy decreases significantly beyond the range of 60 km. Finally, the study compares the performance of 16 stations on LL. The specific results are shown in Figure 8.

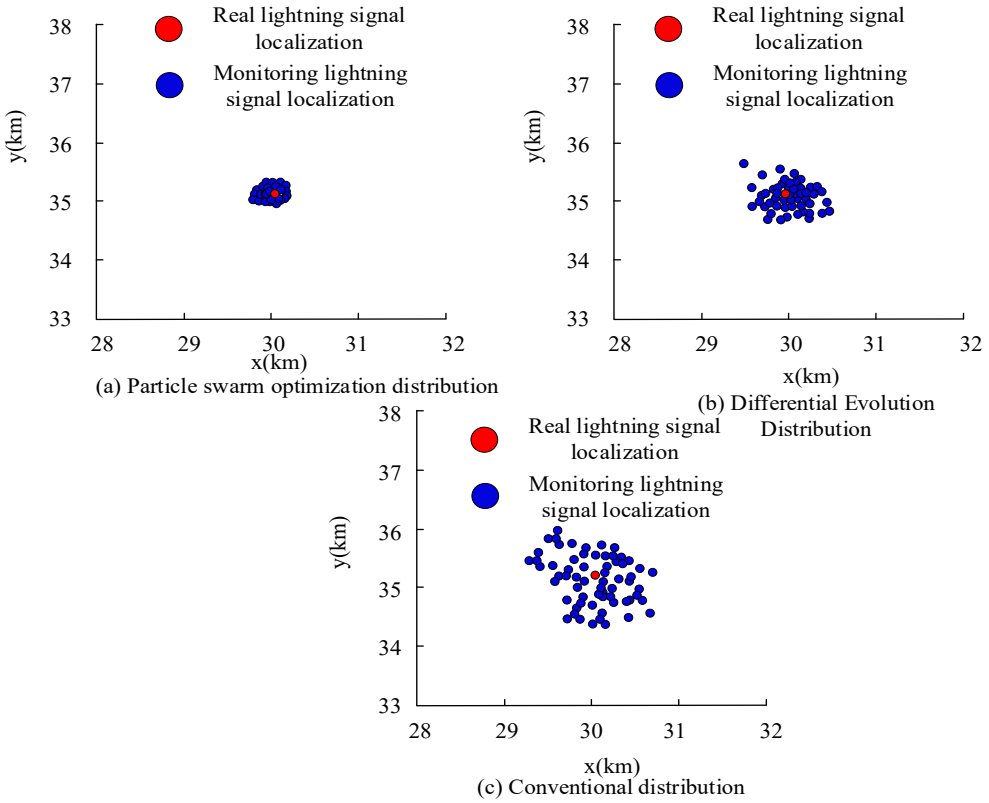

Figure 8. Lightning localization prediction results for 16 sites under different algorithm site distributions.

In Figure 8, when lightning occurs at the coordinates of (30, 35, 10), the 16 sites of PSO locate the lightning signals distributed between 29.6 and 30.3 km on the horizontal axis (HA) and 34.7 and 35.3 km on the vertical axis (VA). The positioning error on the HA and VA is basically less than 0.4 km. On the other hand, the 16 sites of the differential evolutionary algorithm locate the lightning signals in the range of 29.3–30.6 km on the HA and 34.6–35.8 km on the VA. The positioning error on the HA and VA is basically less than 0.7 km. In contrast, under the traditional site distribution method, the 16 sites are distributed between 29.1 and 30.9 km on the HA and 34.2 and 36.1 km on the VA for lightning signal localization. The positioning error on the HA and VA is basically less than 1 km. Therefore, it can be concluded that the PSO model constructed in the study has an advantage in the optimization of the distribution of the 16 sites. The results of site distribution have the smallest error in LL.

5. Conclusions

The study proposes an improved model fusing 3D localization and PSO algorithms for the multi-station distribution of lightning monitoring systems, and the method is validated in experiments. The focus of this study is to construct a relationship model between lightning monitoring station position error and lightning monitoring position error through the arrival angle algorithm and to use the particle swarm optimization algorithm to obtain the optimal lightning monitoring station position distribution with the minimum lightning monitoring position error. In the experiment, the performance of the model was verified through research. In the simulation experiments, PSO completed convergence when the number of iterations reached 90 times, and the solution error was at the level of 0.3 km. Its convergence speed and solving accuracy were basically higher than other algorithm models. Meanwhile, in the four-station distribution simulation, the average error of LL was 0.3267 km under differential evolutionary distribution optimization. Under the distribution optimization of the particle swarm, the average error of LL was 0.3057 km. Therefore, compared to the traditional Y-distribution method, the monitoring station optimized by the differential evolution method partially reduced the lightning positioning error by 42.1%. Compared with the traditional Y-distribution method, the PSO method reduced the lightning positioning error by 45.8%. In addition, in the practical application of 16-station distribution optimization, the positioning error of the research-constructed method was basically less than 0.4 km in the HA and VA. The experiments indicate that the PSO algorithm model constructed by the study has good optimization performance on the distribution of lightning monitoring stations and can improve the positioning accuracy of the lightning monitoring system. The shortcoming of the study is that it considers the factors that affect LL from the perspective of three-dimensional localization but does not explore LL from the perspective of arrival time difference. The direction of future research will also introduce the time difference factor to analyze the factors that influence lightning time difference localization accuracy and the optimization of monitoring station layout.

Author Contributions: Conceptualization, Y.H.; methodology, Y.H.; formal analysis, B.H.; resources, B.H.; data curation, B.H.; writing—original draft preparation, Y.H.; writing—review and editing, H.S. All authors have read and agreed to the published version of the manuscript.

Funding: This study was funded by the National Fund (Research on mechanism and data-driven lightning risk warning for mid and high-voltage overhead power lines 52207109)) and the Major Science and Technology Project of Yunnan Province (Research and application of key technologies for large-scale energy storage to support the high proportion of new energy connected to the power grid in Yunnan (202402AG050006)).

Data Availability Statement: The original contributions presented in the study are included in the article, further inquiries can be directed to the corresponding author.

Conflicts of Interest: The authors declare no conflicts of interest.

References

1. Karami, E.; Khalilinia, A.; Bali, A.; Rouzbehi, K. Monte-Carlo-based simulation and investigation of 230 kV transmission lines outage due to lightning. *High Volt.* **2020**, *5*, 83–91. [CrossRef]
2. Liu, B.; Shi, L.H.; Qiu, S.; Liu, H.Y.; Sun, Z. Three-dimensional lightning positioning in low-frequency band using time reversal in frequency domain. *IEEE Trans. Electromagn. Compat.* **2019**, *62*, 774–784. [CrossRef]
3. Mahomed, M.; Clulow, A.D.; Strydom, S.; Savage, M.J.; Mabhaudhi, T. Lightning monitoring and detection techniques: Progress and challenges in South Africa. *S. Afr. J. Sci.* **2021**, *117*, 1–7. [CrossRef] [PubMed]
4. Xu, X.; Huang, L.; Wang, S.; Ji, Y.; Liu, X.; Fang, G. VLF/LF lightning location based on LWPC and IRI models: A quantitative study. *Remote Sens.* **2022**, *14*, 5784. [CrossRef]

5. Li, W.; Chen, R.; Guo, Y. Closed form algorithm of double-satellite TDOA + AOA localization based on WGS-84 model. *Chin. J. Aeronaut.* **2019**, *32*, 2354–2367. [CrossRef]
6. Chen, Z.; Zhang, Y.; Zheng, D.; Zhang, Y.; Fan, X.; Fan, Y.; Lyu, W. A method of three-dimensional location for LFEDA combining the time of arrival method and the time reversal technique. *J. Geophys. Res. Atmos.* **2019**, *124*, 6484–6500. [CrossRef]
7. Qin, Z.; Chen, M.; Lyu, F.; Cummer, S.A.; Zhu, B.; Liu, F.; Du, Y. A GPU-based grid traverse algorithm for accelerating lightning geolocation process. *IEEE Trans. Electromagn. Compat.* **2019**, *62*, 489–497. [CrossRef]
8. Wang, C.; Ning, Y.; Wang, J.; Zhang, L.; Wan, J.; He, Q. Optimized deployment of anchors based on GDOP minimization for ultra-wideband positioning. *J. Spat. Sci.* **2022**, *67*, 455–472. [CrossRef]
9. Tirkolaee, E.B.; Goli, A.; Mardani, A. A novel two-echelon hierarchical location-allocation-routing optimization for green energy-efficient logistics systems. *Ann. Oper. Res.* **2023**, *324*, 795–823. [CrossRef]
10. Goeritno, A.; Azama, I.M. Explaining the existence of lightning: Literature review and an example of calculating the efficiency value of a detection system. *J. Appl. Sci. Adv. Eng.* **2024**, *2*, 27–36. [CrossRef]
11. Nahar, M.N.; Mostafa, M.G. Statistical characteristics of lightning activities over Bangladesh detected by world wide lightning location network. In Proceedings of the 2024 6th International Conference on Electrical Engineering and Information & Communication Technology (ICEEICT), Dhaka, Bangladesh, 2–4 May 2024; pp. 358–363.
12. Poelman, D.R.; Kohlmann, H.; Schulz, W. Insights into ground strike point properties in Europe through the EUCLID Lightning Location System. *Nat. Hazards Earth Syst. Sci.* **2024**, *24*, 2511–2522. [CrossRef]
13. Wang, P.; Liang, F.; Song, J.; Jiang, N.; Zhang, X.P.; Guo, L.; Gu, X. Impact of the PV location in distribution networks on network power losses and voltage fluctuations with PSO analysis. *CSEE J. Power Energy Syst.* **2020**, *8*, 523–534.
14. Rafi, V.; Dhal, P.K. Maximization savings in distribution networks with optimal location of type-I distributed generator along with reconfiguration using PSO-DA optimization techniques. *Mater. Today Proc.* **2020**, *33*, 4094–4100. [CrossRef]
15. Mehranzamir, K.; Pour, A.B.; Abdul-Malek, Z.; Afrouzi, H.N.; Alizadeh, S.M.; Hashim, M. Implementation of ground-based lightning locating system using particle swarm optimization algorithm for lightning mapping and monitoring. *Remote Sens.* **2023**, *15*, 2306. [CrossRef]
16. Zhang, Y.; Zou, M.; Wang, J.; Li, Y.; Tan, Y.; Zhu, S. Advances in lightning monitoring and location technology research in China. *Remote Sens.* **2022**, *14*, 1293. [CrossRef]
17. Karami, H.; Mostajabi, A.; Azadifar, M.; Rubinstein, M.; Zhuang, C.; Rachidi, F. Machine learning-based lightning localization algorithm using lightning-induced voltages on transmission lines. *IEEE Trans. Electromagn. Compat.* **2020**, *62*, 2512–2519. [CrossRef]
18. Deng, W.; Xu, J.; Zhao, H.; Song, Y. A novel gate resource allocation method using improved PSO-based QEA. *IEEE Trans. Intell. Transp. Syst.* **2020**, *23*, 1737–1745. [CrossRef]
19. Xing, H.; Yang, X.; Zhang, J. Thunderstorm cloud localization algorithm and performance analysis of a three-dimensional atmospheric electric field apparatus. *J. Electr. Eng. Technol.* **2019**, *14*, 2487–2495. [CrossRef]
20. Shuang, J.; Li, H.I.; Yi, C. Accelerate the time-reversal computing of lightning location using GPU and phase-difference filter. *IEEE Trans. Electromagn. Compat.* **2023**, *65*, 496–506.
21. Kumar, M.S.; Mohan, S. Selective fruit harvesting: Research, trends and developments towards fruit detection and localization—A review. *Proc. Inst. Mech. Eng. Part C J. Mech. Eng. Sci.* **2023**, *237*, 1405–1444. [CrossRef]

Disclaimer/Publisher's Note: The statements, opinions and data contained in all publications are solely those of the individual author(s) and contributor(s) and not of MDPI and/or the editor(s). MDPI and/or the editor(s) disclaim responsibility for any injury to people or property resulting from any ideas, methods, instructions or products referred to in the content.